Multi-plasmon effects and plasmon satellites in photoemission from nanostructures

— Electronic Supplementary Information —

P. A. D. Gonçalves[1] and F. Javier García de Abajo[1,2,*]

[1] *ICFO – Institut de Ciències Fotòniques, The Barcelona Institute of Science and Technology, 08860 Castelldefels (Barcelona), Spain*
[2] *ICREA – Institució Catalana de Recerca i Estudis Avançats, Passeig Lluís Companys 23, 08010 Barcelona, Spain*

CONTENTS

I. THEORETICAL FRAMEWORK

We present a comprehensive account of the theoretical framework used in the main text for describing plasmon satellites in core-level photoemission from plasmonic nanostructures. A minimal model governing the electron–plasmon interaction follows from the Hamiltonian [1–5]

$$\hat{\mathcal{H}} = \hbar\omega_0 \hat{a}^\dagger \hat{a} + g^*(t)\,\hat{a}^\dagger + g(t)\,\hat{a}, \tag{S1a}$$

where we assume a single plasmon mode described as a quantum harmonic oscillator, whereas the photoelectron and core hole are treated as classical external charges. More precisely, $\hat{a}^\dagger$ and $\hat{a}$ are bosonic plasmon creation and annihilation operators, ω_0 is the plasmon frequency, and $g(t)$ is a classical time-dependent electron–plasmon coupling energy given by [5]

$$g(t) = \int \mathrm{d}\mathbf{r}\, \phi_\mathrm{p}(\mathbf{r})\, \rho_\mathrm{ext}(\mathbf{r}, t) \tag{S1b}$$

in terms of the electric potential $\phi_\mathrm{p}(\mathbf{r})$ associated with a single plasmon quantum and the combined photoelectron plus core-hole charge density $\rho_\mathrm{ext}(\mathbf{r}, t) = e\left\{\phi_\mathrm{p}(\mathbf{r})\,\delta(\mathbf{r} - \mathbf{r}_0) - \phi_\mathrm{p}(\mathbf{r})\,\delta(\mathbf{r} - [\mathbf{r}_0 + \mathbf{v}t])\right\}\Theta(t)$. Here $\Theta(t)$ is the Heaviside step function and we assume

* javier.garciadeabajo@nanophotonics.es

the photoelectron to be emitted from $\mathbf{r}_0$ at time $t = 0$, following a straight-line trajectory with constant velocity $\mathbf{v}$. Combining this expression and Eq. (S1b), the coupling coefficient can be written as

$$g(t) = [g_0 + g_1(t)]\,\Theta(t) \tag{S2a}$$

in terms of the photohole and photoelectron contributions

$$g_0 \equiv e\phi_\mathrm{p}(\mathbf{r}_0), \tag{S2b}$$

$$g_1(t) \equiv -e\phi_\mathrm{p}(\mathbf{r}_0 + \mathbf{v}t), \tag{S2c}$$

respectively. This model assumes that the core hole is localized and static [6–9], so that the time dependence in $g(t)$ comes from the photoelectron alone.

1. Plasmon eigenstates in the presence of the core hole

The final state of the plasmon at infinite time (i.e., with the photoelectron already far from the structure) is affected by the presence of the photohole. Thus, it is necessary to find the eigenstates of the $t \to \infty$ Hamiltonian

$$\hat{\mathcal{H}}_\infty = \hbar\omega_0 \hat{a}^\dagger \hat{a} + g_0^* \hat{a}^\dagger + g_0 \hat{a}, \tag{S3}$$

which can be readily diagonalized by performing the unitary transformation $\tilde{\mathcal{H}}_\infty = \mathrm{e}^{\hat{s}} \hat{\mathcal{H}}_\infty \mathrm{e}^{-\hat{s}}$ with [6, 10]

$$\hat{s} = \Delta_0^* \hat{a}^\dagger - \Delta_0 \hat{a} \tag{S4}$$

and

$$\Delta_0 = \frac{g_0}{\hbar\omega_0}. \tag{S5}$$

We find

$$\tilde{\mathcal{H}}_\infty = \hbar\omega_0 (\hat{a}^\dagger \hat{a} - |\Delta_0|^2), \tag{S6}$$

and hence

$$\tilde{\mathcal{H}}_\infty |n\rangle = \hbar\omega_0 (n - |\Delta_0|^2)\,|n\rangle\,, \tag{S7}$$

from which we can write

$$\hat{\mathcal{H}}_\infty |\tilde{n}\rangle = \hbar\omega_0 (n - |\Delta_0|^2)\,|\tilde{n}\rangle\,, \tag{S8a}$$

where

$$|\tilde{n}\rangle = \mathrm{e}^{-\hat{s}}\,|n\rangle\,, \tag{S8b}$$

are the sought-after eigenstates with eigenenergies $\hbar\omega_0(n - |\Delta_0|^2)$ corresponding to a rigid shift by $-\hbar\omega_0|\Delta_0|^2$ from the ones of the particle without a hole.

II. PLASMON SATELLITE PROBABILITIES

We calculate the satellite probabilities following a nonperturbative quantum-mechanical approach in two physically relevant scenarios: one in which the plasmon mode is initially in the ground-state (Sec. II A below); and a second one with the plasmon prepared in a coherent state prior to photoemission (e.g., by resonant laser illumination, see Sec. II B). The photoelectron is assumed to be emitted from a core level in a surface atom, which is reasonable considering that the photoelectron escape depth is $\lesssim 1$ nm for kinetic energies in the $10-1500$ eV range [11, 12].

A. Plasmon initially in its ground state

This is a common scenario because we typically have $\hbar\omega_0 \gg k_\mathrm{B}T$, where T is the temperature. The initial plasmon state is $|\psi(t_0 = 0)\rangle = |0\rangle$ and, after photoemission, there is a one-to-one correspondence between the number of plasmons created (n) and the photoelectron energy loss ($n\hbar\omega_0$) relative to the direct peak at kinetic energy E_0. Below, we derive the satellite probabilities using two different (but equivalent) approaches: one based on the coherent-state solution previously identified in the context of electron energy-loss spectroscopy (EELS) [1, 2, 5], and a more general one relying on the S-matrix formalism (bearing some resemblance to the quantum mechanical description of photon-induced near-field electron microscopy (PINEM) [13, 14]).

1. *Coherent-state ansatz*

Noting that the Hamiltonian in Eq. (S1) is the same as for a classically driven quantum harmonic oscillator [15], the Schrödinger equation $\mathrm{i}\hbar|\dot{\psi}(t)\rangle = \hat{\mathcal{H}}\,|\psi(t)\rangle$ admits the solution [5]

$$|\psi(t)\rangle = \mathrm{e}^{\mathrm{i}\chi(t)}\,|\alpha(t)\rangle\,, \tag{S9a}$$

$$|\alpha(t)\rangle = \mathrm{e}^{-|\alpha(t)|^2/2}\sum_{n=0}^{\infty}\frac{[\alpha(t)]^n}{\sqrt{n!}}\mathrm{e}^{-\mathrm{i}n\omega_0 t}\,|n\rangle\,, \tag{S9b}$$

where $|\alpha(t)\rangle$ is a coherent state [obeying $\hat{a}\,|\alpha(t)\rangle = \alpha(t)\,e^{-\mathrm{i}\omega_0 t}\,|\alpha(t)\rangle$] [15, 16] of amplitude

$$\alpha(t) = -\frac{\mathrm{i}}{\hbar}\int_{t_0}^{t}\mathrm{d}t'\,g^*(t')\,\mathrm{e}^{\mathrm{i}\omega_0 t'}, \tag{S10}$$

and $\chi(t) = -\frac{1}{\hbar}\int_{t_0}^{t}\mathrm{d}t'\,\mathrm{Re}\left\{\alpha(t')\,g(t')\,\mathrm{e}^{-\mathrm{i}\omega_0 t'}\right\} + \chi(t_0)$ is a global phase that we ignore in what follows because it does not affect the satellite probabilities.

Projecting Eqs. (S9a) on the eigenstates of Eq. (S8b), the probability associated with a satellite corresponding to the excitation of n plasmons reduces to

$$P_{-n} = |\langle\tilde{n}|\psi(t\to\infty)\rangle|^2 = \lim_{t\to\infty}\,\mathrm{e}^{-|\alpha(t)|^2}\left|\sum_{m=0}^{\infty}\frac{[\alpha(t)]^m}{\sqrt{m!}}\mathrm{e}^{-\mathrm{i}m\omega_0 t}\,M_{nm}\right|^2 \tag{S11a}$$

in terms of the matrix elements

$$M_{nm} = \langle\tilde{n}|m\rangle = \langle n|\,\mathrm{e}^{\hat{s}}\,|m\rangle = \langle n|\,\mathrm{e}^{\Delta_0^*\hat{a}^\dagger - \Delta_0\hat{a}}\,|m\rangle = \mathrm{e}^{-|\Delta_0|^2/2}\,\sqrt{n!m!}\left(\Delta_0^*\right)^{n-m}\sum_{j=\max\{0,m-n\}}^{m}\frac{\left(-|\Delta_0|^2\right)^j}{j!(m-j)!(n-m+j)!} \tag{S11b}$$

[see Appendix A for a detailed derivation of Eq. (S11b)]. Clearly, the probability in Eq. (S11a) is fully characterized by both the quantity $\Delta_0 = g_0/(\hbar\omega_0)$ and the final coherent-state amplitude $\alpha(t\to\infty)$. In particular, combining Eqs. (S1b)–(S2) and (S10), we have

$$\begin{aligned}\alpha(t\to\infty) &= \lim_{t\to\infty}\underbrace{\Delta_0^*\left(1-\mathrm{e}^{\mathrm{i}\omega_0 t}\right)}_{\alpha_0(t)} + \underbrace{\frac{\mathrm{i}e}{\hbar}\int_0^{\infty}\phi_{\mathrm{p}}^*(\mathbf{r}_0+\mathbf{v}t')\,\mathrm{e}^{\mathrm{i}\omega_0 t'}\,\mathrm{d}t'}_{\alpha_1}\\ &= \alpha_0(t) + \alpha_1,\end{aligned} \tag{S12}$$

which is separated into core-hole and photoelectron contributions. Incidentally, there is an apparent dependence on time through $\alpha_0(t)$ in Eq. (S12). However, as we show explicitly in Appendix C, such dependence cancels in P_{-n} when inserting $\alpha(t)$ into Eq. (S11a). Finally, after some algebra, the sought-after probability in Eq. (S11a) reduces to

$$P_{-n} = \frac{|\Delta_0^* + \alpha_1|^{2n}}{n!}\mathrm{e}^{-|\Delta_0^*+\alpha_1|^2} \tag{S13}$$

(see Appendix C for details).

Because the plasmon state before photoemission is empty, the probability of detecting a photoelectron with kinetic energy $E_0 + \ell\hbar\omega_0$, where E_0 is the zero-plasmon photoelectron energy, is given by

$$P_\ell = \frac{|\beta_{\mathrm{PE}}|^{2|\ell|}}{|\ell|!}\mathrm{e}^{-|\beta_{\mathrm{PE}}|^2}\,, \qquad \text{with} \qquad \beta_{\mathrm{PE}} = \Delta_0 + \alpha_1^*, \tag{S14}$$

where $\ell \le 0$ and we have exploited the mapping $n = -\ell$. The probability distribution is thus Poissonian and characterized by an average plasmon population $|\beta_{\mathrm{PE}}|^2$. Incidentally, in the direct peak energy $E_0 = h\nu_X - |E_{\mathrm{B}}| - |g_0|^2/(\hbar\omega_0)$, the difference between the x-ray energy ($h\nu_X$) and the bare core-level energy ($|E_{\mathrm{B}}|$) is shifted by an amount $-|g_0|^2/(\hbar\omega_0)$ due to the photohole–plasmon interaction (relaxation shift).

2. *Time-evolution operator: S-matrix formalism*

The S-matrix formalism provides an alternative way of deriving the satellite probabilities that proves to be advantageous when introducing optical pumping (see Sec. II B below). In the interaction picture, the time dependence of the wave function follows from the unitary transformation $|\psi_{\rm I}(t)\rangle = {\rm e}^{{\rm i}\hat{\mathcal{H}}_{0,{\rm S}}t/\hbar}\,|\psi_{\rm S}(t)\rangle$, where $|\psi_{\rm S}(t)\rangle$ and $\hat{\mathcal{H}}_{0,{\rm S}} = \hbar\omega_0\hat{a}^\dagger\hat{a}$ are, respectively, the wave function and the free Hamiltonian in the Schrödinger picture [17]. Then, the Schrödinger equation transforms to ${\rm i}\hbar|\dot{\psi}_{\rm I}(t)\rangle = \hat{\mathcal{H}}_{1,{\rm I}}\,|\psi_{\rm I}(t)\rangle$ in the interaction picture, where $\hat{\mathcal{H}}_{1,{\rm I}} = {\rm e}^{{\rm i}\hat{\mathcal{H}}_{0,{\rm S}}t/\hbar}\,\hat{\mathcal{H}}_{1,{\rm S}}\,{\rm e}^{-{\rm i}\hat{\mathcal{H}}_{0,{\rm S}}t/\hbar} = g^*(t)\,{\rm e}^{{\rm i}\omega_0 t}\hat{a}^\dagger + g(t)\,{\rm e}^{-{\rm i}\omega_0 t}\hat{a}$. The dynamic evolution of the wave function can be conveniently described in terms of the time-evolution or scattering-matrix operator $\hat{S}(t,t_0) = \exp\left\{-({\rm i}/\hbar)\int_{t_0}^{t}{\rm d}t'\hat{\mathcal{H}}_{1,{\rm I}}(t')\right\}$ via $|\psi_{\rm I}(t)\rangle = \hat{S}(t,t_0)\,|\psi_{\rm I}(t_0)\rangle$. In the present instance, the S-matrix takes the form [2, 14, 15, 18]

$$\hat{S}(t,t_0) = {\rm e}^{{\rm i}\chi_{\rm I}(t,t_0)}\,{\rm e}^{\beta^*(t,t_0)\hat{a}^\dagger - \beta(t,t_0)\hat{a}}, \tag{S15a}$$

where

$$\beta(t,t_0) = \frac{\rm i}{\hbar}\int_{t_0}^{t}{\rm d}t'\,g(t')\,{\rm e}^{-{\rm i}\omega_0 t'}, \tag{S15b}$$

and $\chi_{\rm I}(t,t_0)$ is a global phase that can be ignored in the context of this work. To calculate the satellite probabilities, we need the matrix elements $\langle n|\,\hat{S}(t,t_0)\,|m\rangle$, which admit the analytical form [2, 14, 15, 18]

$$S_{nm}(\beta) \equiv \langle n|\,\hat{S}(t,t_0)\,|m\rangle = {\rm e}^{{\rm i}\chi_{\rm I}}\,{\rm e}^{-|\beta|^2/2}\,\sqrt{n!m!}\,\big(\beta^*\big)^{n-m}\sum_{j=\max\{0,m-n\}}^{m}\frac{\big(-|\beta|^2\big)^j}{j!(m-j)!(n-m+j)!}, \tag{S16}$$

as obtained from analogous calculations to those for M_{nm} in Eq. (S11b) and Appendix A. When starting from the ground state ($m = 0$), Eq. (S16) takes a simple form that can also be found by exploiting the fact that $\hat{S} = {\rm e}^{{\rm i}\chi_{\rm I}}\hat{D}(\beta^*)$ is essentially the displacement operator $\hat{D}(\beta^*) = \exp\{\beta^*(t,t_0)\hat{a}^\dagger - \beta(t,t_0)\hat{a}\}$, and thus, we find $\hat{S}\,|0\rangle = {\rm e}^{{\rm i}\chi_{\rm I}}\,|\beta^*\rangle$, leading to $S_{m0} = {\rm e}^{{\rm i}\chi_{\rm I}}\,\langle m|\beta^*\rangle = {\rm e}^{{\rm i}\chi_{\rm I}}{\rm e}^{-|\beta^*|^2}\,(\beta^*)^m/\sqrt{m!}$.

Given the initial condition $|\psi_{\rm S}(t_0 = 0)\rangle = |0\rangle$ (i.e., $|\psi_{\rm I}(t_0 = 0)\rangle = |0\rangle$), we have $|\psi_{\rm I}(t)\rangle = \hat{S}(t,0)\,|0\rangle$, and thus, the satellite probability is obtained from

$$\begin{aligned}
P_{-n} = |\langle\tilde{n}|\psi_{\rm S}(t\to\infty)\rangle|^2 &= \lim_{t\to\infty}\left|\langle\tilde{n}|\,{\rm e}^{-{\rm i}\hat{H}_0 t/\hbar}\,|\psi_{\rm I}(t)\rangle\right|^2\\
&= \lim_{t\to\infty}\left|\langle\tilde{n}|\,{\rm e}^{-{\rm i}\hat{H}_0 t/\hbar}\hat{S}(\infty,0)\,|0\rangle\right|^2\\
&= \lim_{t\to\infty}\left|\sum_{m=0}^{\infty}\langle\tilde{n}|\,\underbrace{{\rm e}^{-{\rm i}\hat{H}_0 t/\hbar}\,|m\rangle}_{{\rm e}^{-{\rm i}m\omega_0 t}\,|m\rangle}\langle m|\,\hat{S}(\infty,0)\,|0\rangle\right|^2\\
&= \lim_{t\to\infty}\left|\sum_{m=0}^{\infty}{\rm e}^{-{\rm i}m\omega_0 t}M_{nm}\,S_{m0}\right|^2\\
&= \lim_{t\to\infty}\,{\rm e}^{-|\beta(t)|^2}\left|\sum_{m=0}^{\infty}\frac{[\beta^*(t)]^m}{\sqrt{m!}}{\rm e}^{-{\rm i}m\omega_0 t}\,M_{nm}\right|^2,
\end{aligned} \tag{S17}$$

which coincides with Eq. (S11a), noting that $\beta(t) \equiv \beta(t,0) = \alpha^*(t)$ [cf. (S10) and (S15b)]. Then, the satellite probability reduces again to Eq. (S14).

B. Plasmon initially in a coherent state: Illuminated sample

When the plasmon mode is prepared in a coherent state by external optical pumping prior to photoemission, the satellite probabilities can be readily calculated using the S-matrix formalism following the same procedure as in Sect. II A 2, but with an initial plasmon state $|\psi_{\rm I}(0)\rangle = \sum_{n_0=0}^{\infty}c_{n_0}\,|n_0\rangle$, with coefficients $c_{n_0} = {\rm e}^{-\bar{n}_0/2}\,\bar{n}_0^{n_0/2}/\sqrt{n_0!}$ determined by the average plasmon

population $\bar{n}_0$. The phase in c_{n_0} is irrelevant because each plasmon Fock state leads to mutually orthogonal final photoelectron–plasmon states, so we set it to zero. Then, repeating the same steps as in Eq. (S17), we find the matrix elements

$$\begin{aligned}\langle\tilde{n}|\psi_S(t\to\infty)\rangle &= \lim_{t\to\infty}\langle\tilde{n}|\,\mathrm{e}^{-\mathrm{i}\hat{H}_0 t/\hbar}\,|\psi_1(t)\rangle \\ &= \lim_{t\to\infty}\sum_{n_0=0}^{\infty} c_{n_0}\,\langle\tilde{n}|\,\mathrm{e}^{-\mathrm{i}\hat{H}_0 t/\hbar}\hat{S}\,(\infty,0)\,|n_0\rangle \\ &= \lim_{t\to\infty}\sum_{n_0=0}^{\infty} c_{n_0}\sum_{m=0}^{\infty}\mathrm{e}^{-\mathrm{i}m\omega_0 t}\,\langle\tilde{n}|m\rangle\,\langle m|\,\hat{S}\,(\infty,0)\,|n_0\rangle \\ &= \lim_{t\to\infty}\sum_{n_0=0}^{\infty} c_{n_0}\sum_{m=0}^{\infty}\mathrm{e}^{-\mathrm{i}m\omega_0 t}M_{nm}\,S_{mn_0}. \end{aligned} \tag{S18}$$

The unpumped scenario is readily recoved by setting $c_{n_0} = \delta_{n_0,0}$. Under pumping, the amplitudes in Eq. (S18) allow us to write the photoemission spectral probability as

$$\Gamma(E) = \sum_{\ell=-\infty}^{\infty} P_\ell\,\delta(E - E_0 - \ell\hbar\omega_0), \tag{S19a}$$

where E is the photoelectron kinetic energy, and

$$P_\ell = \sum_{n=\max\{0,-\ell\}}^{\infty}\left|f_\ell^n\right|^2 \tag{S19b}$$

is the probability associated with satellite ℓ (i.e., photoelectrons that have changed their energy by $\ell\hbar\omega_0$ with respect to the direct peak at E_0), expressed in terms of the squared amplitudes

$$\left|f_\ell^n\right|^2 = \left|\lim_{t\to\infty} c_{n+\ell}\sum_{m=0}^{\infty}\mathrm{e}^{-\mathrm{i}m\omega_0 t}M_{n,m}(\Delta_0)\,S_{m,n+\ell}[\beta(t)]\right|^2. \tag{S19c}$$

Here, we have made the dependences of the matrix elements of M and $\hat{S}$ explicit [recall that $\beta(t\to\infty) \equiv \Delta_0(1-\mathrm{e}^{-\mathrm{i}\omega_0 t}) + \beta_1(\infty)$] and used the fact that the number of excitations in the photoelectron–sample system is conserved (i.e., $n_0 = n + \ell$) [14, 18]. We remark that time enters Eq. (S19c) through the explicit exponential and also through $\hat{S}\,(t,0)$, which depends on $\beta(t)$, although the overall expression is time-independent at long times [i.e., just like Eq. (S17) becomes Eq. (S14), as explicitly shown in Appendix C]. We have verified this property upon numerical inspection. An analytical proof of this time-independence comes from the fact that the coupling coefficient β_1 (which characterizes the photoelectron–plasmon interaction) can be formulated in terms of the mode electric field in a way analogous to PINEM (see next section), where $\left|f_\ell^n\right|^2$ takes an analytical form that coincides with $\left|S_{n,n+\ell}(\beta)\right|^2$ using the $\hat{S}$ coefficients defined in Eq. (S16) [14]. This result should be reproduced by Eq. (S19c) when $M_{n,m} = \delta_{m,n}$ (i.e., without post-interaction plasmon state mixing $\langle\tilde{n}|m\rangle$, as no photohole is involved in PINEM). We thus argue that $\left|\mathrm{e}^{-\mathrm{i}m\omega_0 t}S_{m,n+\ell}[\beta(t)]\right|^2$ is a time-independent quantity given by $|S_{n,n+\ell}(\beta_1)|^2$ [i.e., Eq. (S16), evaluated by replacing $\beta\to\beta_1$] (i.e., time independent). Consequently, Eq. (S19c) can be expressed as

$$\left|f_\ell^n\right|^2 = \left|c_{n+\ell}\sum_{m=0}^{\infty}M_{n,m}(\Delta_0)\,S_{m,n+\ell}(\beta_1)\right|^2. \tag{S20}$$

From here, and noting that both matrix elements $M_{i,j}$ and $S_{i,j}$ stem from displacement operators [namely, $\mathrm{e}^{\hat{s}}$ and $\hat{S}$; recall Eqs. (S11b) and (S16)], and that the sum in the preceding equation is nothing but $\mathrm{e}^{\mathrm{i}\chi_1}\langle n|\,\hat{D}(\Delta_0^*)\hat{D}(\beta_1^*)\,|n+\ell\rangle = \mathrm{e}^{\mathrm{i}\chi_1}\mathrm{e}^{\mathrm{i}\,\mathrm{Im}\{\Delta_0^*\beta_1\}}\,\langle n|\,\hat{D}(\beta_{\mathrm{PE}}^*)\,|n+\ell\rangle$, we can write

$$\left|f_\ell^n\right|^2 = \left|c_{n+\ell}\,S_{n,n+\ell}(\beta_{\mathrm{PE}})\right|^2, \tag{S21}$$

as presented in the main text.

C. Equivalence of the potential and electric-field descriptions in the quasistatic limit

As outlined above, the plasmon satellite probabilities can be calculated using Eqs. (S14) and (S19b), which depend on the key parameter $\beta_{\mathrm{PE}} = \Delta_0 + \alpha_1^*$. The specific particle geometry and composition determines the plasmon frequency ω_0 and the single-plasmon electrostatic potential $\phi_{\mathrm{p}}(\mathbf{r})$, from which the two terms in these parameters are obtained as

$$\Delta_0 = \frac{g_0}{\hbar\omega_0} = \frac{e\phi_{\mathrm{p}}(\mathbf{r}_0)}{\hbar\omega_0}, \tag{S22}$$

and

$$\alpha_1^* = \beta_1 = -\frac{\mathrm{i}e}{\hbar}\int_0^\infty \phi_{\mathrm{p}}(\mathbf{r}_0 + \mathbf{v}t)\,\mathrm{e}^{-\mathrm{i}\omega_0 t}\mathrm{d}t. \tag{S23}$$

We now show that a description of the electron–plasmon interaction in terms of the single-plasmon electric field yields identical results as the one above relying on the potential.

For simplicity, we focus on the unexcited particle and assume that the photoelectron is emitted along z (i.e., $\mathbf{v} = v\,\hat{\mathbf{z}}$) with the hole placed at z_0. Omitting the explicit dependence of the potential on (x, y), we have

$$\beta_1 = -\frac{\mathrm{i}e}{\hbar v}\int_{z_0}^\infty \phi_{\mathrm{p}}(z)\,\mathrm{e}^{-\mathrm{i}\omega_0(z-z_0)/v}\mathrm{d}z.$$

Noting that this equation can be rearranged as

$$\begin{aligned}
\beta_1 &= \mathrm{e}^{\mathrm{i}\omega_0 z_0/v}\frac{e}{\hbar\omega_0}\int_{z_0}^\infty \mathrm{d}z\,\phi_{\mathrm{p}}(z)\,\frac{\partial}{\partial z}\left(\mathrm{e}^{-\mathrm{i}\omega_0 z/v}\right)\\
&= \mathrm{e}^{\mathrm{i}\omega_0 z_0/v}\frac{e}{\hbar\omega_0}\Bigg[\underbrace{\phi_{\mathrm{p}}(z)\,\mathrm{e}^{-\mathrm{i}\omega_0 z/v}\Big|_{z_0}^\infty}_{-\phi_{\mathrm{p}}(z_0)\,\mathrm{e}^{-\mathrm{i}\omega_0 z_0/v}} - \int_{z_0}^\infty \mathrm{d}z\ \underbrace{\frac{\partial\phi_{\mathrm{p}}(z)}{\partial z}}_{\simeq -E_z(z)}\ \mathrm{e}^{-\mathrm{i}\omega_0 z/v}\Bigg]\\
&= -\frac{e\phi_{\mathrm{p}}(z_0)}{\hbar\omega_0} + \frac{e}{\hbar\omega_0}\,\mathrm{e}^{\mathrm{i}\omega_0 z_0/v}\int_{z_0}^\infty \mathrm{d}z\,E_z(z)\,\mathrm{e}^{-\mathrm{i}\omega_0 z/v}\\
&= -\Delta_0 + \frac{e}{\hbar\omega_0}\,\mathrm{e}^{\mathrm{i}\omega_0 z_0/v}\int_{z_0}^\infty \mathrm{d}z\,E_z(z)\,\mathrm{e}^{-\mathrm{i}\omega_0 z/v},
\end{aligned}$$

we find

$$\beta_{\mathrm{PE}} = \Delta_0 + \beta_1 = \frac{e}{\hbar\omega_0}\int_{z_0}^\infty E_z(z)\,\mathrm{e}^{-\mathrm{i}\omega_0(z-z_0)/v}\,\mathrm{d}z. \tag{S24}$$

This is precisely the coupling parameter that one obtains from a description of the electron–plasmon interaction in terms of the normalized electric field, which has been extensively used in PINEM [13, 14] for free electrons, with the difference that in that case the lower limit of integration is extended to $z_0 \to -\infty$. Equation (S24) further demonstrates that the potential and electric-field formulations lead to identical results.

III. PLASMON SATELLITES IN PHOTOEMISSION FROM METAL NANOPARTICLES

We now apply the above formalism to metallic nanoparticles, illustrated by an analytical treatment of spheres and a more general approach based on numerical electromagnetic solvers for arbitrary shapes. In all cases, we consider the particle size to be small enough to justify the application of the quasistatic limit. Nevertheless, retardation effects affecting the LSP resonance and the corresponding electric field can still be incorporated using the electric field description outlined in Sect. II C to calculate the coupling parameter from Eq. (S24) that determines the satellite probabilities in the absence [Eq. (S14)] or presence [Eqs. (S19b) and (S21)] of external pumping.

A. Homogeneous nanosphere

We consider a metallic nanosphere of radius R hosting a dominant dipolar plasmon. For simplicity, we discuss the interaction with a photoelectron emitted along the z direction from a surface point $\mathbf{r}_0 = (0, 0, R)$ [i.e., $z_0 = R$], such that only the plasmon mode with polarization along z interacts with the photoelectron. For a dipolar mode, the potential outside the sphere can generally be written as

$$\phi_{\rm p}(\mathbf{r}) = \frac{\mathbf{p}\cdot\mathbf{r}}{r^3} = \frac{p\,z}{r^3} \tag{S25}$$

in terms of a dipole moment $\mathbf{p} = p\hat{z}$. From here, we find the parameter [see Eq. (S5)]

$$\Delta_0 = \frac{ep}{\hbar\omega_0 R^2}. \tag{S26}$$

Neglecting inelastic losses, the metal is well-described in terms of a Drude-like dielectric function $\epsilon_{\rm m}(\omega) = \epsilon_{\rm b} - \omega_{\rm p}^2/\omega^2$ with parameters $\epsilon_{\rm b} = 4$ and $\hbar\omega_{\rm p} = 9.17\,$eV for silver [19, 20]. Then, for the homogeneous sphere the single-plasmon normalization condition sets the value of the dipole moment to (see Appendix B)

$$p = \sqrt{\frac{3\hbar\omega_0}{2}\frac{R^3}{\epsilon_{\rm b}+2}}, \tag{S27}$$

where the mode frequency is given by $\omega_0 = \omega_{\rm p}/\sqrt{\epsilon_{\rm b}+2}$. Combining Eqs. (S26) and (S27), we obtain

$$\Delta_0 = \sqrt{\frac{\alpha\,\hbar c}{2R\,\hbar\omega_0}\frac{3}{\epsilon_{\rm b}+2}}, \tag{S28}$$

where $\alpha \simeq 1/137$ is the fine-structure constant. Furthermore, from Eqs. (S23) and (S25), changing the integration variable to $\tau = \omega_0 t' = \omega_0(z - z_0)/v$, we find

$$\beta_1 = -\mathrm{i}\Delta_0\, a^2 \int_0^\infty \mathrm{d}\tau \frac{\mathrm{e}^{-\mathrm{i}\tau}}{(a+\tau)^2}\,, \qquad \text{where} \qquad a \equiv \frac{\omega_0 R}{v}. \tag{S29}$$

Solving the integral, we find the solution

$$\beta_1 = -\mathrm{i}\Delta_0 F(a), \tag{S30a}$$

where

$$F(a) = a^2 \int_0^\infty \mathrm{d}\tau \frac{\mathrm{e}^{-\mathrm{i}\tau}}{(a+\tau)^2} = a - a^2\,\mathrm{e}^{\mathrm{i}a}\left[\pi - \mathrm{i}\,\mathrm{Ei}(-\mathrm{i}a)\right], \tag{S30b}$$

and $\mathrm{Ei}(z)$ denotes the exponential integral function [21]. Finally, combining the results in Eqs. (S28) and (S30), the photoemission coupling parameter is found to be

$$\beta_{\rm PE} = \Delta_0 + \beta_1 = \Delta_0\left\{1 - \mathrm{i}a + a^2\,\mathrm{e}^{\mathrm{i}a}\left[\mathrm{i}\pi + \mathrm{Ei}(-\mathrm{i}a)\right]\right\}. \tag{S31}$$

Based on this expression, we plot in Fig. S1 the plasmon satellite probabilities from metallic nanospheres (solid curves), as compared with the sudden limit approximation (dashed lines, $\beta_{\rm PE} = \Delta_0$), which is smoothly approached as the photoelectron velocity raises and a becomes increasingly small.

B. Nanoshell

We now consider a metallic spherical shell of inner and outer radii $R_{\rm i}$ and R, respectively, whose core is characterized by a dielectric of permittivity $\epsilon_{\rm c}$. The analytical results for the homogeneous sphere directly apply to the nanoshell, except that the mode frequency and single-plasmon dipole moment are now dependent on the ratio $x \equiv R_{\rm i}/R$ and the core permittivity. Using an analytical expression for the electrostatic polarizability of a nanoshell [22], we find two dipolar plasmon modes (bonding and

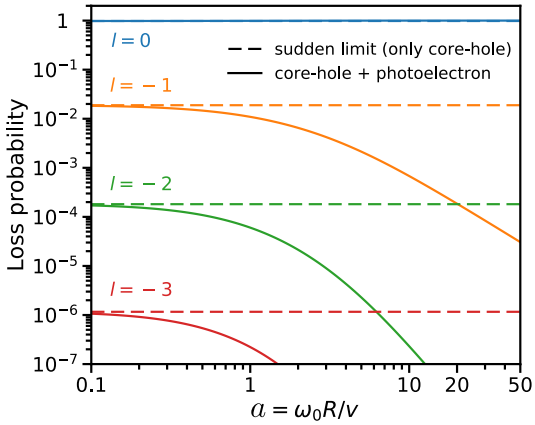

Fig. S1. Plasmon satellite probabilities in core-level photoemission associated with the simultaneous excitation of $n = -\ell$ plasmons in a silver sphere of radius $R = 5$ nm, initially prepared with $n = 0$. We compare the probabilities calculated in the sudden approximation [i.e., only including the hole–plasmon interaction, dashed lines, Eq. (S14) with $\beta_{\rm PE} = \Delta_0$] with those obtained by including the photoelectron–plasmon interaction as well [solid curves, Eq. (S14)].

anti-bonding) of frequencies subject to the condition $[2\epsilon_{\rm m}(\omega) + \epsilon_{\rm c}][\epsilon_{\rm m}(\omega) + 2] = 2x^3\,[\epsilon_{\rm m}(\omega) - \epsilon_{\rm c}][\epsilon_{\rm m}(\omega) - 1]$. We concentrate on the lowest LSP frequency ω_0, for which we obtain

$$p = \sqrt{\hbar\omega_{\rm p}\, R^3\, f(x)}, \tag{S32}$$

which combined with Eq. (S26) leads to

$$\Delta_0 = \sqrt{\frac{\alpha\,\hbar c}{R\,\hbar\omega_0}\,\frac{\omega_{\rm p}}{\omega_0}\,f(x)}. \tag{S33}$$

Here,

$$f(x) = \frac{\left[(2\epsilon_{\rm b} + \epsilon_{\rm c})\Omega_0^2 - 2\right]\left[(\epsilon_{\rm b} - 1)\Omega_0^2 - 1\right] - x^3\left[(\epsilon_{\rm b} - \epsilon_{\rm c})\Omega_0^2 - 1\right]\left[(2\epsilon_{\rm b} + 1)\Omega_0^2 - 2\right]}{2\Omega_0\sqrt{8\,(x^3-1)\,(AB - 2CDx^3) + (A + 2B - 2[C + D]x^3)^2}},$$

with $\Omega_0 = \omega_0/\omega_{\rm p}$, $A = 2\epsilon_{\rm b} + \epsilon_{\rm c}$, $B = \epsilon_{\rm b} + 2$, $C = \epsilon_{\rm b} - \epsilon_{\rm c}$, $D = \epsilon_{\rm b} - 1$, and the metal described by the same Drude-like permittivity as in the homogeneous sphere.

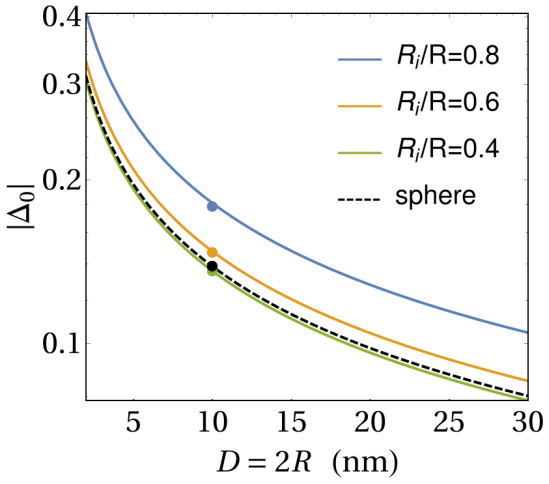

Fig. S2. Comparison between the analytical result [lines, via Eq. (S33), lines] for the photohole–plasmon coupling parameter $|\Delta_0|$ and the same obtained via full retarded numerical solution based on the boundary-element method [color-matched data-points, via $|\Delta_0| = |e\phi_{\rm p}(R)|/(\hbar\omega_0)$, see Sect. III C below], corresponding to silver core-shell nanoparticles with metallic shells of different thicknesses but same outer radius $R = 5$ nm.

C. Small particles of arbitrary shape

Thus far, we have restricted our analysis to spherical nanoparticles for which we find closed-form analytical solutions in the quasistatic limit. For arbitrarily shaped nanoparticles, we use an alternative approach to determine the eigenfield/eigenpotential normalization constant by using numerical electromagnetic solvers and proceeding along the following steps:

1. We numerically compute the EELS probability distribution $\Gamma^{\rm num}_{\rm EELS}(\omega)$ corresponding to a swift electron passing near the nanoparticle, adapting the solver parameters (e.g., symmetry restrictions) and trajectory characteristics such that only the mode that is targeted is contributes to the EELS probability. Additionally, the spectrum directly yields the plasmon frequency ω_0.

2. We fit a Lorentzian distribution profile $\mathcal{L}(\omega) = \dfrac{A}{\pi}\dfrac{\gamma/2}{(\omega_0-\omega)^2+(\gamma/2)^2}$ to $\Gamma^{\rm num}_{\rm EELS}(\omega)$ (with fitting parameters ω_0, A, and γ) and determine the total EELS probability through $P^{\rm num}_{\rm EELS} = \int_0^\infty {\rm d}\omega\, \Gamma^{\rm num}_{\rm EELS}(\omega) \approx \int_0^\infty {\rm d}\omega\, \mathcal{L}(\omega)$ ($\approx A$ for $\gamma \ll \omega_0$). This Lorentzian fitting facilitates the integration over $\omega \in [0,\infty)$.

3. Noting that the total EELS probability in the weak-coupling regime is also given by (see Appendix B) $P_{\rm EELS} = |\alpha_{\rm EELS}|^2 \simeq \left|\dfrac{e}{\hbar\omega_0}\displaystyle\int_{-\infty}^{\infty} {\rm d}z\, E_z(z)\, {\rm e}^{-{\rm i}\omega_0 z/v}\right|^2$, we find a normalization constant $\mathcal{N}$ via $\int_0^\infty {\rm d}\omega\, \mathcal{L}(\omega) = \left|\frac{e}{\hbar\omega_0}\int_{-\infty}^{\infty} {\rm d}z\, \mathcal{N} E^{\rm num}_z(z)\, {\rm e}^{-{\rm i}\omega_0 z/v}\right|^2$, where $E^{\rm num}_z(z)$ is the z-component of the induced electric field produced upon irradiation by a light plane wave polarized along that direction. In these expressions, we assume the photoelectron velocity and the mode polarization to be both parallel to z as well.

4. Using the value of $\mathcal{N}$ found in the previous step, we calculate the coupling coefficient $\beta_{\rm PE}$ from Eq. (S24) by plugging the normalized mode field $E_z(z) = \mathcal{N} E^{\rm num}_z(z)$. We also obtain $\Delta_0 = e\phi_{\rm p}(z_0)/\hbar\omega_0$ [see Eq. (S22)] from the potential at the core, which is computed from $\phi_{\rm p}(z_0) = \int_{z_0}^\infty dz\, E_z(z)$.

Appendix A: Derivation of Eq. (S11b)

The computation of the matrix elements $M_{nm} \equiv \langle \tilde{n}|m\rangle = \langle n|\, {\rm e}^{\hat{s}}\, |m\rangle$ in Eq. (S11b) follows from

$$
\begin{aligned}
M_{nm} = \langle n|\, {\rm e}^{\hat{s}}\, |m\rangle &= \langle n|\, {\rm e}^{\Delta_0^* \hat{a}^\dagger - \Delta_0 \hat{a}}\, |m\rangle \\
&\overset{\rm (i)}{=} e^{-|\Delta_0|^2/2}\, \langle n|\, {\rm e}^{\Delta_0^* \hat{a}^\dagger} e^{-\Delta_0 \hat{a}}\, |m\rangle \\
&\overset{\rm (ii)}{=} e^{-|\Delta_0|^2/2} \sum_{k=0}^{n}\sum_{j=0}^{m} \frac{(\Delta_0^*)^k (-\Delta_0)^j}{k!\, j!} \sqrt{\frac{n!m!}{(n-k)!(m-j)!}}\, \underbrace{\langle n-k|m-j\rangle}_{\delta_{n-k,m-j}},
\end{aligned}
$$

where the last expression can be readily arranged into the form of Eq. (S11b). In step (i) of the above derivation, we have used the Baker–Hausdorff formula [23] ${\rm e}^{\hat{A}+\hat{B}} = {\rm e}^{\hat{A}}\, {\rm e}^{\hat{B}}\, {\rm e}^{-\frac{1}{2}[\hat{A},\hat{B}]}$, valid for any pair of noncommuting operators $\hat{A}$, $\hat{B}$ satisfying $[\hat{A},[\hat{A},\hat{B}]] = [\hat{B},[\hat{A},\hat{B}]] = 0$, and here specified for $\hat{A} \equiv \Delta_0^* \hat{a}^\dagger$ and $\hat{B} \equiv -\Delta_0 \hat{a}$. In step (ii), we have carried out the calculations

$$
e^{-\Delta_0 \hat{a}}\, |m\rangle = \sum_{j=0}^{\infty} \frac{(-\Delta_0)^j}{j!} \hat{a}^j\, |m\rangle = \sum_{j=0}^{m} \frac{(-\Delta_0)^j}{j!} \sqrt{\frac{m!}{(m-j)!}}\, |m-j\rangle\,, \qquad m \geq j,
$$

and

$$
\langle n|\, {\rm e}^{\Delta_0^* \hat{a}^\dagger} = \left(e^{\Delta_0 \hat{a}}\, |n\rangle\right)^\dagger = \sum_{k=0}^{n} \frac{(\Delta_0^*)^k}{k!} \sqrt{\frac{n!}{(n-k)!}}\, \langle n-k|\,, \qquad n \geq k.
$$

Appendix B: Normalization of the single-plasmon potential

In the quasistatic regime, the plasmon mode potential and its corresponding normalization for one quantum can be obtained, for instance, through classical electrostatic theory based on a modal expansion [2, 3, 24]. Depending on the nanoparticle morphology, the electrostatic eigenmodes and eigenfrequencies can be found either analytically [24] or numerically [25, 26]. The potential associated with a single optical excitation then follows from imposing the appropriate bosonic commutation relations in the standard way [2, 24].

Alternatively, if the electrostatic eigemodes are known only up to a constant (i.e., not normalized), an alternative strategy to find the correct normalization consists in comparing the quantum-mechanical EELS probability in the weak-coupling regime with

the total (i.e., spectrally integrated) classical electron energy-loss probability [14]. Here, we follow this approach, whose details are outlined below for a dipolar mode of a nanosphere. The analysis is similar for other morphologies.

A quantum mechanical description of the electron–plasmon interaction in the context of EELS has been previously worked out [1–3, 5] following similar steps as in Secs. I and II. More specifically, in the weak-coupling regime—wherein the electron loses a single quantum of energy associated with the excitation of a single plasmon—and assuming an initially depleted optical mode, the quantum mechanical EELS probability is given by

$$P_{\text{EELS}} = |\alpha_{\text{EELS}}|^2 \qquad \text{where} \qquad \alpha_{\text{EELS}} = \frac{\mathrm{i}e}{\hbar}\int_{-\infty}^{\infty} \mathrm{d}t\, \mathrm{e}^{\mathrm{i}\omega_0 t}\, \phi_{\text{p}}^*[\mathbf{r}_e(t)], \tag{B1}$$

with the coherent-state amplitude $\alpha_{\text{EELS}} \equiv \alpha(t \to \infty, t_0 \to -\infty)$ obtaind by using the coupling energy in Eq. (S1b) with $g(t) = \int \mathrm{d}\mathbf{r}\phi_{\text{p}}(\mathbf{r})\,\{-e\delta(\mathbf{r} - \mathbf{r}_e[t])\}$.

For an electric dipolar mode in a sphere, the associated potential can be written as

$$\phi_{\text{p}}(\mathbf{r}) = \frac{\mathbf{p}\cdot\mathbf{r}}{r^3}$$

in terms of the transition-dipole moment $\mathbf{p}$. Considering a swift single electron moving with constant velocity v along the straight trajectory $\mathbf{r}_e(t) = b\,\hat{\mathbf{x}} + vt\,\hat{\mathbf{z}}$ and passing at a distance b from the center of a self-standing nanosphere of radius R, we have

$$\alpha_{\text{EELS}} = \frac{\mathrm{i}e}{\hbar v}\int_{-\infty}^{\infty} \mathrm{d}z\, \mathrm{e}^{\mathrm{i}\omega_0 z/v}\, \frac{p_x^* b + p_z^* z}{\left[b^2 + z^2\right]^{3/2}}.$$

By changing the integration variable to $u = \omega_0 z/v$, this expression can be recast into[1]

$$\begin{aligned}\alpha_{\text{EELS}} &= \frac{\mathrm{i}e\omega_0}{\hbar v^2}\left\{p_x^*\int_{-\infty}^{\infty}\mathrm{d}u\frac{\bar{b}\,\mathrm{e}^{\mathrm{i}u}}{\left[\bar{b}^2+u^2\right]^{3/2}} + p_z^*\int_{-\infty}^{\infty}\mathrm{d}u\frac{u\,\mathrm{e}^{\mathrm{i}u}}{\left[\bar{b}^2+u^2\right]^{3/2}}\right\}\\ &= \frac{\mathrm{i}e\omega_0}{\hbar v^2}\left\{p_x^*\, 2K_1(\bar{b}) + p_z^*\, 2\mathrm{i}K_0(\bar{b})\right\},\end{aligned} \tag{B2}$$

where $\bar{b} = \omega_0 b/v$, and $K_\nu(x)$ is the modified Bessel function of the second kind of order ν [21]. Finally, because the sphere is isotropic, we actually need to sum the contributions of the electron interaction with three dipolar modes having orthogonal polarizations (i.e., $p\hat{\mathbf{x}}$, $p\hat{\mathbf{y}}$, and $p\hat{\mathbf{z}}$, respectively), leading to the EELS probability

$$P_{\text{EELS}} = |\alpha_{\text{EELS}}|^2 = \left|p\frac{2e\omega_0}{\hbar v^2}\right|^2\left[K_0^2\left(\bar{b}\right) + K_1^2\left(\bar{b}\right)\right]. \tag{B3}$$

This expression can now be compared to the well-known result from classical quasistatic dielectric theory for a metallic sphere of radius R and permittivity $\epsilon_{\text{m}}(\omega)$ [27],

$$\Gamma_{\text{EELS}}(\omega) = \frac{4\alpha c\omega^2 R^3}{\pi v^4}\left[K_0^2\left(\bar{b}\right) + K_1^2\left(\bar{b}\right)\right]\mathrm{Im}\left\{\frac{\epsilon_{\text{m}}(\omega)-1}{\epsilon_{\text{m}}(\omega)+2}\right\}, \tag{B4}$$

and then, the total EELS probability is given by

$$P_{\text{EELS}} = \int_0^\infty \mathrm{d}\omega\, \Gamma_{\text{EELS}}(\omega). \tag{B5}$$

We describe the metal through the Drude-like permittivity $\epsilon_{\text{m}}(\omega) = \epsilon_{\text{b}} - \omega_{\text{p}}^2/\omega(\omega + \mathrm{i}\gamma)$ in the lossless limit $\gamma \to 0$ with parameters depending on the type of metal (e.g., $\epsilon_{\text{b}} = 4$ and $\hbar\omega_{\text{p}} = 9.17\,\text{eV}$ for silver [19, 20]). Using this expression, we have $\mathrm{Im}\left\{\frac{\epsilon_{\text{m}}(\omega)-1}{\epsilon_{\text{m}}(\omega)+2}\right\} \to \frac{\pi\omega_0}{2}\frac{3}{\epsilon_{\text{b}}+2}\delta(\omega-\omega_0)$, where the mode frequency $\omega_0 = \omega_{\text{p}}/\sqrt{\epsilon_{\text{b}}+2}$ comes from the pole at $\epsilon_{\text{m}}(\omega) = -2$ in the expressions above. Inserting this limit in Eqs. (B4) and (B5), we readily obtain

$$P_{\text{EELS}} = \frac{2\alpha c\omega_0^3 R^3}{v^4}\frac{3}{\epsilon_{\text{b}}+2}\left[K_0^2\left(\bar{b}\right) + K_1^2\left(\bar{b}\right)\right]. \tag{B6}$$

Finally, Eqs. (B3) and (B6) are identical when the mode dipole is set to the value indicated in Eq. (S27), which agrees with the single-quantum normalization found in the literature [3, 24].

---

[1] In the second step, from the integral representation of the modified Bessel functions of the second kind [21] $K_\nu(z) = \frac{\Gamma(\nu+\frac{1}{2})}{\sqrt{\pi}}(2z)^\nu\int_0^\infty \mathrm{d}t\frac{\cos t}{\left[z^2+t^2\right]^{\nu+1/2}}$, we find $\int_{-\infty}^{\infty}\mathrm{d}u\frac{\bar{b}\,\mathrm{e}^{\mathrm{i}u}}{\left[\bar{b}^2+u^2\right]^{3/2}} = 2K_1(\bar{b})$ and $\int_{-\infty}^{\infty}\mathrm{d}u\frac{u\,\mathrm{e}^{\mathrm{i}u}}{\left[\bar{b}^2+u^2\right]^{3/2}} = -\int_{-\infty}^{\infty}\mathrm{d}u\,\mathrm{e}^{\mathrm{i}u}\frac{\partial}{\partial u}\left(\frac{1}{\sqrt{\bar{b}^2+u^2}}\right) = \mathrm{i}\int_{-\infty}^{\infty}\mathrm{d}u\frac{\mathrm{e}^{\mathrm{i}u}}{\sqrt{\bar{b}^2+u^2}} = 2\mathrm{i}K_0(\bar{b})$.

Appendix C: Derivation of Eq. (S13)

Using Eqs. (S11) and (S12), we can write

$$
\begin{aligned}
P_{-n} &= \mathrm{e}^{-|\alpha_0(t)+\alpha_1|^2}\left|\sum_{m=0}^{\infty}\frac{[\alpha_0(t)+\alpha_1]^m}{\sqrt{m!}}\mathrm{e}^{-\mathrm{i}m\omega_0 t}\,M_{nm}\right|^2 \\
&= \mathrm{e}^{-|\alpha_0(t)+\alpha_1|^2}\mathrm{e}^{-|\Delta_0|^2}n!\,|\Delta_0|^{2n}\left|\sum_{m=0}^{\infty}\left(\frac{[\alpha_0(t)+\alpha_1]\,\mathrm{e}^{-\mathrm{i}\omega_0 t}}{\Delta_0^*}\right)^m\sum_{j=\max\{0,m-n\}}^{m}\frac{\left(-|\Delta_0|^2\right)^j}{j!(m-j)!(n-m+j)!}\right|^2 \\
&= \mathrm{e}^{-|\alpha_0(t)+\alpha_1|^2}\mathrm{e}^{-|\Delta_0|^2}n!\,|\Delta_0|^{2n}\left|\sum_{j=0}^{\infty}\sum_{m=j}^{j+n}\left(\frac{[\alpha_0(t)+\alpha_1]\,\mathrm{e}^{-\mathrm{i}\omega_0 t}}{\Delta_0^*}\right)^m\frac{\left(-|\Delta_0|^2\right)^j}{j!(m-j)!(n-m+j)!}\right|^2,
\end{aligned}
\tag{C1}
$$

where we have rearranged the double-sum $\sum_{m=0}^{\infty}\sum_{j=\max\{0,m-n\}}^{m}$ as $\sum_{j=0}^{\infty}\sum_{m=j}^{j+n}$ in the last step. Next, defining $x \equiv -|\Delta_0|^2$ and $y \equiv [\alpha_0(t)+\alpha_1]\,\mathrm{e}^{-\mathrm{i}\omega_0 t}/\Delta_0^* = \alpha(t)\,\mathrm{e}^{-\mathrm{i}\omega_0 t}/\Delta_0^*$ (for shorthand notation), we have

$$
\begin{aligned}
P_{-n} &= \mathrm{e}^{-|\alpha(t)|^2}\mathrm{e}^{-|\Delta_0|^2}n!\,|\Delta_0|^{2n}\left|\sum_{j=0}^{\infty}\sum_{m=j}^{j+n}\frac{x^j\,y^m}{j!(m-j)!(n-m+j)!}\right|^2 \\
&\overset{1}{=} \mathrm{e}^{-|\alpha(t)|^2}\mathrm{e}^{-|\Delta_0|^2}n!\,|\Delta_0|^{2n}\left|\sum_{j=0}^{\infty}\frac{(x\,y)^j}{j!}\frac{1}{n!}\sum_{k=0}^{n}\frac{n!}{k!(n-k)!}y^k\right|^2 \\
&\overset{2}{=} \mathrm{e}^{-|\alpha(t)|^2}\mathrm{e}^{-|\Delta_0|^2}n!\,|\Delta_0|^{2n}\left|\frac{(1+y)^n}{n!}\sum_{j=0}^{\infty}\frac{(x\,y)^j}{j!}\right|^2 \\
&\overset{3}{=} \frac{1}{n!}\,\mathrm{e}^{-|\alpha(t)|^2}\mathrm{e}^{-|\Delta_0|^2}\,|\Delta_0|^{2n}\,|(1+y)^n\,\mathrm{e}^{xy}|^2 \\
&\overset{4}{=} \frac{1}{n!}\,\mathrm{e}^{-|\alpha(t)|^2}\mathrm{e}^{-|\Delta_0|^2}\,|\Delta_0|^{2n}\left|1+\frac{\alpha(t)\,\mathrm{e}^{-\mathrm{i}\omega_0 t}}{\Delta_0^*}\right|^{2n}\exp\left(-2\,\mathrm{Re}\left\{\Delta_0\,\alpha(t)\,\mathrm{e}^{-\mathrm{i}\omega_0 t}\right\}\right),
\end{aligned}
\tag{C2}
$$

where we have proceeded along the following steps:

1. Redefining the sum over m through the transformation $k \to m-j$.
2. Using the binomial formula $\sum_{k=0}^{n}\frac{n!}{k!(n-k)!}y^k = (1+y)^n$.
3. Identifying the power-series definition of the exponential function.
4. Converting back to the original variables.

After some simple algebraic manipulations, Eq. (C2) can be written in the form

$$
P_{-n} = \frac{1}{n!}\left|\Delta_0^* + \alpha(t)\,\mathrm{e}^{-\mathrm{i}\omega_0 t}\right|^{2n}\exp\left(-\left|\Delta_0^* + \alpha(t)\,\mathrm{e}^{-\mathrm{i}\omega_0 t}\right|^2\right).
\tag{C3}
$$

Now, recalling [e.g., from Eq. (S12)] that $\alpha(t) = \alpha_0(t)+\alpha_1 = \Delta_0^*\left(1-\mathrm{e}^{\mathrm{i}\omega_0 t}\right)+\alpha_1$, we have

$$
\begin{aligned}
\left|\Delta_0^* + \alpha(t)\,\mathrm{e}^{-\mathrm{i}\omega_0 t}\right|^2 &= \left|\Delta_0^* + \Delta_0^*(\mathrm{e}^{-\mathrm{i}\omega_0 t}-1) + \alpha_1\,\mathrm{e}^{-\mathrm{i}\omega_0 t}\right|^2 \\
&= \left|(\Delta_0^* + \alpha_1)\,\mathrm{e}^{-\mathrm{i}\omega_0 t}\right|^2 \\
&= \left|\Delta_0^* + \alpha_1\right|^2,
\end{aligned}
$$

and thus, Eq. (C3) translates into the time-independent result in Eq. (S13).

SUPPLEMENTARY REFERENCES

[1] A. A. Lucas and M. Šunjić, Prog. Surf. Sci. **2**, 75 (1972).
[2] A. A. Lucas, E. Kartheuser, and R. G. Badro, Phys. Rev. B **2**, 2488 (1970).
[3] T. L. Ferrell and P. M. Echenique, Phys. Rev. Lett. **55**, 1526 (1985).
[4] L. Hedin, J. Michiels, and J. Inglesfield, Phys. Rev. B **58**, 15565 (1998).
[5] F. J. García de Abajo, ACS Nano **7**, 11409 (2013).
[6] D. C. Langreth, Phys. Rev. B **1**, 471 (1970).
[7] G. D. Mahan, phys. stat. sol. (b) **55**, 703 (1973).
[8] J. W. Gadzuk, J. Electron Spectrosc. Relat. Phenom. **11**, 355 (1977).
[9] J. E. Inglesfield, J. Phys. C: Solid State Phys. , 403 (1983).
[10] G. D. Mahan, *Many-particle Physics*, 3rd ed. (Springer, New York, 2000).
[11] S. Hüfner, *Photoelectron Spectroscopy: Principles and Applications*, 3rd ed. (Springer-Verlag, 2003).
[12] M. P. Seah and W. A. Dench, Surf. Interface Anal. **1**, 2 (1979).
[13] F. J. García de Abajo and V. Di Giulio, ACS Photonics **8**, 945 (2021).
[14] V. Di Giulio, M. Kociak, and F. J. García de Abajo, Optica **6**, 1524 (2019).
[15] P. Carruthers and M. M. Nieto, Am. J. Phys. **33**, 537 (1965).
[16] R. J. Glauber, Phys. Rev. **131**, 2766 (1963).
[17] J. J. Sakurai, *Modern Quantum Mechanics* (Addison-Wesley, 1994).
[18] V. Di Giulio and F. J. García de Abajo, Optica **7**, 1820 (2020).
[19] P. B. Johnson and R. W. Christy, Phys. Rev. B **6**, 4370 (1972).
[20] R. Yu, L. M. Liz-Marzán, and F. J. García de Abajo, Chem. Soc. Rev. **46**, 6710 (2017).
[21] M. Abramowitz and I. A. Stegun, *Handbook of Mathematical Functions* (Dover, New York, 1972).
[22] V. Myroshnychenko, J. Rodríguez-Fernández, I. Pastoriza-Santos, A. M. Funston, C. Novo, P. Mulvaney, L. M. Liz-Marzán, and F. J. García de Abajo, Chem. Soc. Rev. **37**, 1792 (2008).
[23] M. O. Scully and M. S. Zubairy, *Quantum Optics* (Cambridge University Press, Cambridge, 1997).
[24] R. Brako, J. Hrnčević, and M. Šunjić, Z. Phys. B: Condens. Matter Quanta **21**, 193 (1975).
[25] F. Ouyang and M. Isaacson, Philos. Mag. B **60**, 481 (1989).
[26] F. J. García de Abajo and J. Aizpurua, Phys. Rev. B **56**, 15873 (1997).
[27] F. J. García de Abajo, Rev. Mod. Phys. **82**, 209 (2010).